Micropatterned Nanocomposite Hydrogels for Biosensing Applications

Valber A. Pedrosa,[a, b] *Jun Yan*,[c] *Aleksandr L. Simonian*,*[a] *Alexander Revzin**[c]

[a] Department of Materials Engineering, Auburn University, Auburn, AL 36849, USA
[b] Current address: Institute of Bioscience, Department of Chemistry and Biochemistry, UNESP, Botucatu, SP, Brazil
[c] Department of Biomedical Engineering, University of California, Davis, 451 Health Sciences St. #2619, Davis, CA 95616, USA
*e-mail: als@eng.auburn.edu; arevzin@ucdavis.edu

Received: October 23, 2010
Accepted: December 18, 2020

Abstract
This paper describes the use of Au nanoparticle (NP)-containing hydrogel microstructures in the development of electrochemical enzyme-based biosensors. To fabricate biosensors, AuNPs were conjugated with glucose oxidase (GOX) or horseradish peroxidase (HRP) molecules and were dispersed in the prepolymer solution of poly(ethylene glycol) diacrylate (PEG-DA). Vinylferrocene (VF) was also added into the prepolymer solution in order to lower operating potential of the biosensor and to prevent oxidation of interfering substances. The prepolymer solution was photolithographically patterned in alignment with an array of Au electrodes fabricated on glass. As a result, electrode arrays became functionalized with AuNP/GOX- or AuNP/HRP-carrying hydrogel microstructures. Performance of the biosensors was characterized by impedance spectroscopy, chronoapmerometry and cyclic voltammetry. Impedance measurements revealed that inclusion of Au nanoparticles improved conductivity of PEG hydrogel by a factor of 5. Importantly, biosensors based on AuNP-GOX complex exhibited high sensitivity to glucose ($100\ \mu A\,mM^{-1}\,cm^{-2}$) in the linear range from 0.1 to 10 mM. The detection limit was estimated to be 3.7×10^{-7} M at a signal-to-noise ratio of 3. Biosensors with immobilized AuNP/HPR had a linear response from 0.5 to 5.0 μM of hydrogen peroxide with sensitivity of $1.4\ mA\,mM^{-1}\,cm^{-2}$. The method for fabricating nanoparticle-carrying hydrogel microstructures described in this paper should be widely applicable in the development of robust and sensitive electrochemical biosensors.

Keywords: Glucose oxidase, Gold nanoparticles, Hydrogel, HPR

DOI: 10.1002/elan.201000654

1 Introduction

Integration of biorecognition and signal transduction elements has been an important area of biosensors research for several decades. Recent attention has turned towards employment of nanostructures to enhance functionality of biosensors [1–4]. Au nanoparticles are one of the most studied and most attractive types of nanomaterials due to their excellent conductivity and chemical stability [4–6]. Au nanoparticles are easy to functionalize and can serve as scaffolds for immobilization of biomolecules during biosensor fabrication [7–9]. Significantly, Au nanoparticles have been shown to enhance electron transfer from a prosthetic group of an oxidoreductase enzyme to an electrode, resulting in higher sensitivity of analyte detection [4,6].

Metal nanoparticles are frequently incorporated into polymeric matrices to create biosensors [10–12]. For example, nanoparticles have been physically entrapped inside stimuli-responsive gels, providing a change in optical [13] or electrical signal [14] upon phase transition of the gel. An approach most commonly used for creating electrochemical biosensors involves electrodeposition of a conductive polymer from nanoparticle-containing solution [8,15,16].

Hydrogels comprised of poly(ethylene glycol) (PEG) possess a number of properties making them attractive for biosensor fabrication. PEG hydrogels have been shown to be excellent matrices for entrapment of biomolecules [17–19]. These hydrogels are non-fouling and can therefore help eliminate biosensor fouling in complex solutions such as physiological fluids or cell culture media [20,21]. In addition, PEG hydrogels may be micropatterned in a manner similar to photolithography [18,22]. Leveraging these advantages, our laboratory has recently described fabrication of electrochemical biosensors by immobilizing enzyme- and redox molecule-carrying hydrogel microstructures on top of Au microelectrode arrays [23]. These biosensors were successfully used to detect glucose and lactate, however, their sensitivity was considerably lower than some of the best glucose biosensors reported in the literature (glucose sensitivity of $0.9\ \mu A\,mM^{-1}\,cm^{-2}$ in our previous study [23] vs. 20 to $500\ \mu A\,mM^{-1}\,cm^{-2}$ in other reports [24,25]).

In the present study, we wanted to incorporate AuNPs into hydrogel microstructures in order to increase sensi-

tivity of the biosensor. We hypothesized that AuNP would serve a dual purpose of enhancing conductivity of the hydrogel and improving electron transfer from enzyme to the electrode. To test this hypothesis, AuNPs were conjugated with GOX or HRP molecules via standard alkanethiols chemistry and were incorporated into hydrogel microstructures along with vinyl ferrocene (VF) redox molecules. These sensing hydrogels were microfabricated on top of Au electrode arrays and were characterized using impedance spectroscopy, chronoamperometry and cyclic voltammetry. Impedance spectroscopy revealed that hydrogels containing AuNP-GOX were 5 times more conductive than hydrogels with GOX alone. Importantly, AuNP-containing biosensors showed sensitivity of 100 $\mu A\,mM^{-1}\,cm^{-2}$ and lower limit of detection of 0.3 μM glucose. Inclusion of VF redox molecules further enhanced electron transfer through the gel and allowed to operate under lower oxidation potentials to avoid interfering substances such as uric and ascorbic acids. The strategy for integrating nanoparticle-carrying hydrogels onto miniature electrodes described in this paper should be broadly applicable in construction of robust and sensitive enzyme-based biosensors.

2 Experimental

2.1 Materials

Poly (ethylene glycol) diacrylate (PEG-DA, MW 575), 2-hydroxy-2methyl-propiophenone (photoinitiator), 99.9% toluene, glucose oxidase (GOX) (EC 1.1.3.4, type II-S from *Aspergillus niger* (18000 $U\,g^{-1}$ solid), horseradish peroxidase (HRP) (EC 1.11.1.7, type VI-A), *N*-hydroxysuccinimide (NHS), 1-ethyl-3-(3-dimethylaminopropyl) carbodiimide (EDC), D-(+)-glucose, hydrogen peroxide, and vinylferrocene (VF) were purchased from Sigma (St Louis, MO, USA). AuNPs was purchased from BB international (Cardiff, UK). Diameter of AuNPs was 15 nm. Phosphate buffered saline (PBS) 10 mM was used as a supporting electrolyte for all experiments and flow injection analysis experiments. Water used for preparation of aqueous solutions came from a Millipore Direct-Q water purification system (resistivity, 18 $M\Omega\,cm^{-2}$). D-(+)-glucose solutions were allowed to mutarotate overnight at room temperature before use. Stock solutions were prepared in bi-distilled water or buffer solution and stored in the dark at 4 °C.

2.2 Equipment

All electrochemistry experiments were performed using a CH Instruments (CH1910B) bi-potentiostat. All experiments were conducted in a three electrode system containing a platinum wire auxiliary electrode, working electrode and a saturated Ag/AgCl (3 M) reference electrode. The buffer solution (10 mM PBS) was deoxygenated with pure N_2 for 10 minutes before measurements. All electrochemical measurements were performed at room temperature.

Transmission Electron Microscopy (TEM) samples were prepared by placing a drop of gold nanoparticle dispersion on 200 mesh formvar coated nickel grids and air-dried overnight before imaging. Images were recorded by a Zeiss EM 10 transmission electron microscope operating at 60 kV. The UV-vis spectra at different stages of AuNP modification were collected using Ultrospec 2100 pro from GE life science (Piscataway, NJ, USA) with a 1 cm quartz cell.

2.3 Preparation of Enzyme-Modified AuNPs

The MUA-modified AuNPs were prepared by ligand exchange between mercapto-carboxylic acid (MUA) and citrate-stabilized AuNPs, following previous reported protocols [30]. Scheme 1 shows steps required for conjugation of enzyme molecules onto AuNPs. In a typical experiment, 1.0 mL suspension of Au nanoparticle was gently added to 1.0 mL MUA solution (1 mM in 70% of Ethanol and 30% of water) and vigorously stirred for 4 h. Subsequently, the mixture was centrifuged to remove excess alkanethiol and resuspended in phosphate buffer (10 mM, pH 6.5). Attachment of enzyme molecules

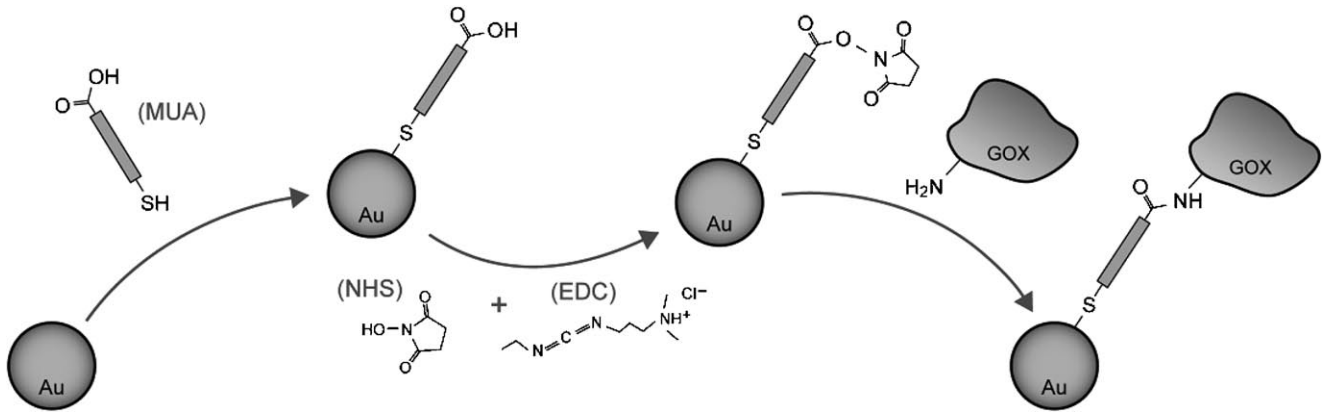

Scheme 1. Conjugation of enzyme molecules to AuNPs. The same approach was used for HRP and GOX attachment to nanoparticles.

(GOX or HRP) to MUA/AuNP was carried out using standard EDC/NHS conjugation chemistry. Briefly, 1 mL AuNP solution were incubated with 100 mM NHS and 200 mM EDC solution for 2 h under stirring, then added to 100 μL GOX or HRP solution (15 mg mL^{-1} in 10 mM of PBS at pH 6.0) and stirred overnight.

2.4 Fabricating AuNP/GOX Carrying Hydrogel Microstructures on Top of Electrode Arrays

Arrays of gold electrodes were fabricated on glass using standard photoresist lithography and wet etching approaches. Each array consisted of 5 electrodes, 300 μm in diameter each, connected to 2×2 mm square contact pads via 15 μm wide leads. The design of the electrode array is described in greater detail in our previous publication [23].

Prepolymer solution contained PEG-DA and 2% (v/v) photoinitiator (2-hydroxy-2-methyl-propiophenone). 10 μL enzyme-modified AuNPs were mixed with 50 μL PEG/vinylferrocene (10 mg/mL) by sonication for 1 min and then stirred overnight at 4 °C. The PEG prepolymer solution containing AuNPs and redox species was photopolymerized on top of the Au electrodes in a process similar to photolithography (see Figure 1). Briefly, PEG-based prepolymer solution was spin-coated at 800 rpm for 4 s onto glass slides containing Au electrode patterns. A photomask was registered with an electrode pattern and then exposed to UV light at 65 mW/cm^2 for 10 s to convert liquid prepolymer into cross-linked hydrogel. The surfaces were developed in DI water for 3 min to remove unpolymerized PEG precursor solution. Enzyme carrying hydrogel microstructures were made larger than Au electrodes; feature sizes were 600 and 300 μm diameter for hydrogel elements and Au electrodes respectively. This was done to ensure effective anchoring of the hydrogel structures to silanized glass substrates.

2.5 Electrochemical Characterization of Sensing Electrodes

Electrodes were tested in a custom-made electrochemical cell with a volume of ca. 1 mL. 1xPBS (pH 7) was degassed with N_2 for ca. 15 min prior to all experiments. Cyclic voltammetry and chronoamperometry were used to characterize response of electrochemical biosensors to glucose. The anodic potential of VF redox molecules entrapped in the PEG hydrogel was determined to be ca. 0.35 V (vs. Ag/AgCl) by cyclic voltammetry. Therefore, during amperometric detection glucose or hydrogen peroxide, hydrogel-modified Au electrodes were poised at 0.35 V. Glucose or hydrogen peroxide aliquots of known concentration were introduced into the electrochemical cell after the background current stabilized. Fabricated sensors were stored in the refrigerator at 4 °C prior to use.

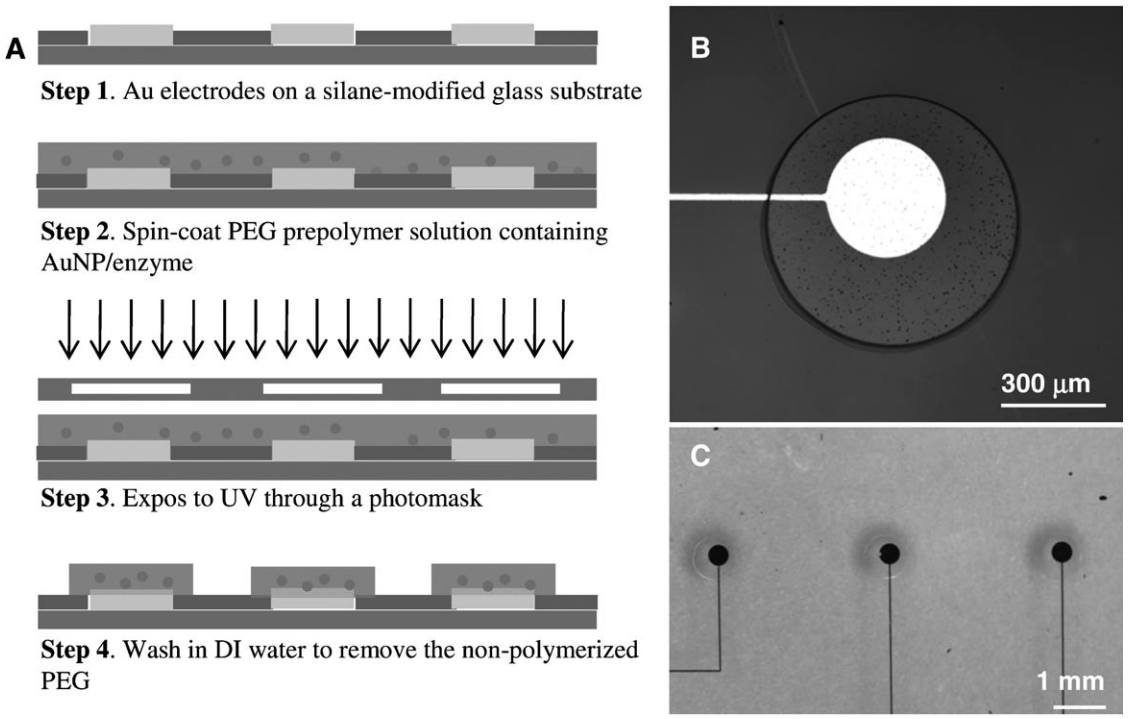

Fig. 1. A) Process flow diagram for patterning nanocomposite hydrogels on Au electrode arrays. B, C) Brightfield images of typical hydrogel/Au electrode used in the studies. 300 μm diameter Au electrode covered with 600 μm diameter nancomposite hydrogel disk is shown in (B). An array of three electrodes with immobilized hydrogel disks is shown in in (C). AuNP/enzyme conjugates were entrapped inside hydrogel microstructures and immobilized onto Au electrode arrays.

Impedance spectroscopy measurements were made using a μAutolab Type III/FRA2 response analyzer (Eco Chemie BV) with a frequency range of 0.001–10 Hz and signal amplitude of 5 mV. The experiments were carried out in a 1.0×10^{-3} M ferrocenemethanol (FeMeOH) in aqueous solution of 0.1 M KCl. All impedance spectra were fitted to equivalent electrical circuits using FRA2 software.

3 Results and Discussion

3.1 Conjugation of Enzymes to AuNPs

This paper describes the use of nanoparticle- and enzyme-carrying hydrogels in the development of electrochemical biosensors. AuNPs were conjugated with GOX or HRP and were immobilized on top of electrode arrays using PEG hydrogel photolithography. The resultant biosensors were found to be sensitive and specific to glucose and hydrogen peroxide.

In order to conjugate enzyme molecules, AuNP were first modified with mercaptoundecanoic acid (MUA) so as to introduce COOH moieties as shown in Scheme 1. UV-vis spectroscopy was used to characterize modification of AuNPs. Figure 2 shows UV-vis spectra of AuNP at different stages of surface modification. For HRP alone, the spectra exhibit characteristic Soret band around 500 nm, and a weak Q band around 400 and 650 nm [26]. The wavelength of the heme band maxima is 500 nm in PBS at pH 6.5. As can be seen in Figure 2A (curve 1), an absorption band of 515 nm was associated with bare AuNPs. After modification with MUA (curve 2) there was a small 10 nm shift in the band associated with AuNP and also a decrease in the absorption peak intensity. This may be interpreted as MUA assembling and creating a dielectric layer on AuNPs. Modification of thiolated AuNPs with EDC/NHS resulted in a further shift of 60 nm (see curve 3 in Figure 2). This behavior has been reported in prior studies describing modification of AuNPs [27] and may be attributed to partial aggregation of the nanoparticles. Incubation of AuNPs in HRP-containing solution leads to the appearance of new adsorption peaks at 410 and 650 nm, which correspond to Soret and weak Q bands of HRP and point towards enzyme conjugation onto AuNPs [27,28].

AuNPs were characterized by TEM (see Figure 2B) and were found to be well dispersed with individual particle diameter of ca. 15 nm. After alkanethiol and HRP modification, the particle diameter increased to ca. 30–50 nm. This change in particle size could be attributed to the assembly of MUA and HRP molecules on AuNPs [29].

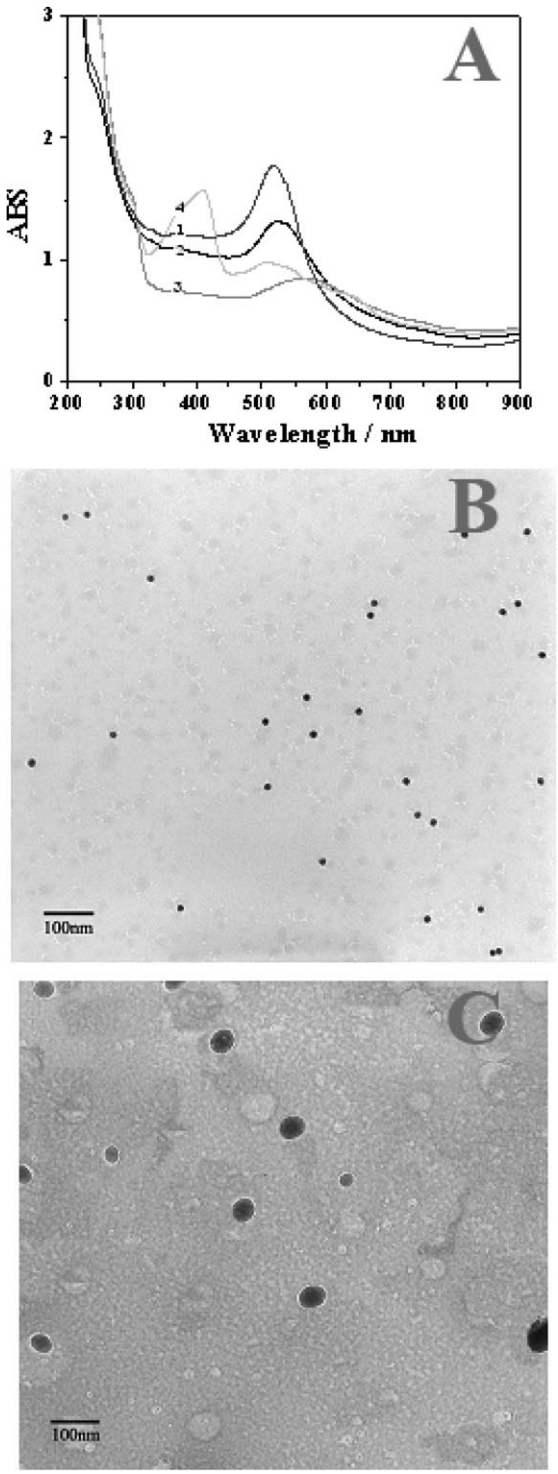

Fig. 2. A) UV-vis spectra of 1) AuNP, 2) MUA modified AuNP, 3) EDC/NHS-activated AuNPS and 4) the HRP/AuNP bioconjugates, B) TEM images of Gold nanoparticle and C) the HRP/AuNP bioconjugates.

3.2 Enhancement of Charge Transport in AuNP-Containing Hydrogels

We hypothesized that inclusion of AuNPs should improve conductivity of PEG hydrogels. To test this hypothesis electrode arrays functionalized with nanocomposite hydrogels were characterized by chronoamperometry and impedance spectroscopy. Figure 3A shows chronoamperometric transient upon the application of a potential step from −0.3 V to 0.3 V to an electrode modified with PEG/

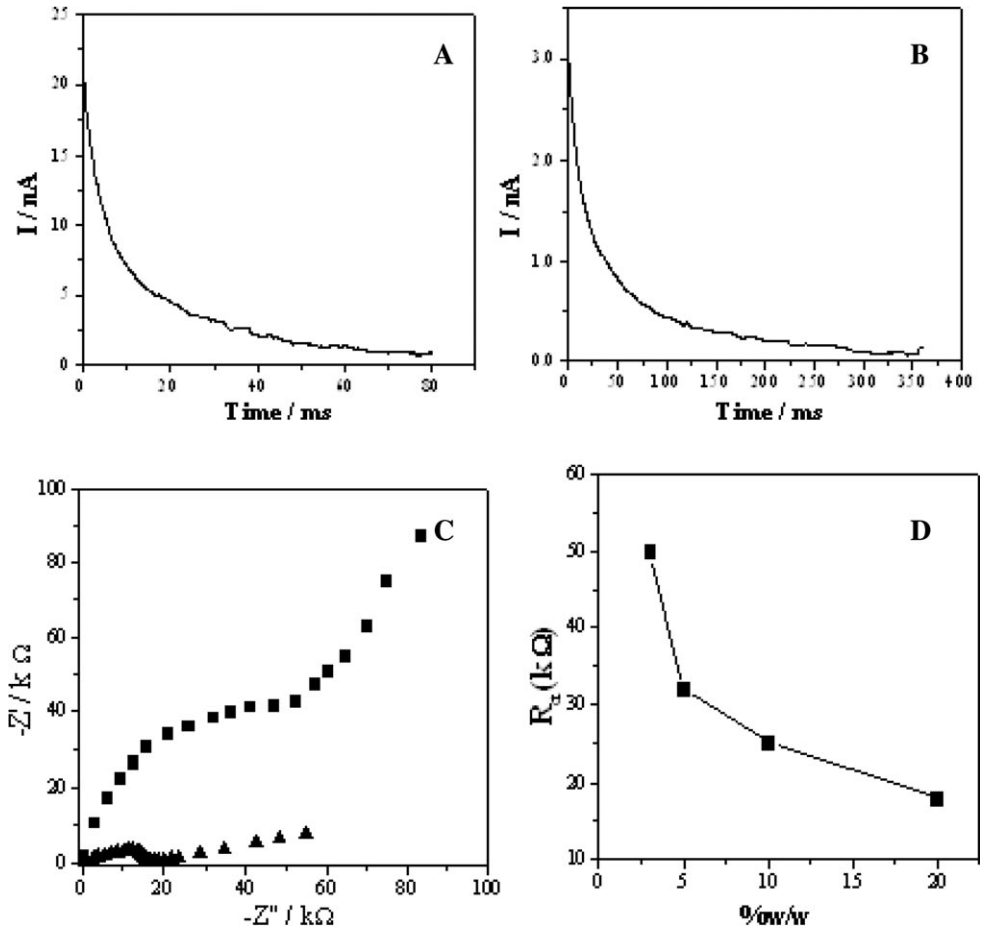

Fig. 3. A, B) Chronoamperometric transients measured after applying a step in potential from −0.3 V to 0.3 V to electrodes modified with hydrogels containing AuNP/GOX (A) and PEG/GOX (B). C) Impedance spectroscopy of nanocomposite hydrogel/Au electrodes. Nyquist plots for hydrogel/Au electrodes containing PEG/GOX (■) and PEG/AuNP/GOX (▲). Experiments performed in 1 mM FcMeOH dissolved in aqueous solution of 0.1 M KCl. Frequency intervals were from 50 kHz to 30 mHz and measurements were carried out at 0.35 V vs. Ag/AgCl. D) Impedance measurements as a function of AuNP loading into hydrogels. Loading refers to concentration of AuNP in liquid prepolymer prior to UV exposure and cross-linking.

AuNP/GOX-containing hydrogel. In this electrode the anodic current transient decayed within ca. 80 ms. For comparison, Figure 3B shows the anodic current transient observed for PEG/GOX modified electrode at the same potential step. The current transient in this system decayed substantially slower – within ca. 330 ms. These results indicate faster electron transfer in AuNP-containing hydrogel microstructures.

To corroborate chronoamperometry results, nanocompostive hydrogels were analyzed by impedance spectroscopy. (EIS) measurements were performed in the presence of a redox molecule FeMeOH (dissolved in 0.1 M KCl). EIS is an effective tool for studying interfacial properties of modified electrodes [30,31]. The semicircle diameters of EIS spectra are related to electron-transfer resistance where the diameter of the semicircle represents charge-transfer resistance (R_{ct}) at the electrode surface. Figure 3C compares the electrochemical impedance spectra (Nyquist plots, Z″ vs. Z′) for hydrogels with and without AuNPs. As seen from these data, the diameter of the semicircle or charge transfer resistance R_{ct}, decreases in presence of gold nanoparticle, suggesting that gold AuNPs facilitate electron transfer through the hydrogel. The values for charge transfer resistance were determined to be 18 kΩ for PEG/AuNP/GOX and 90 kΩ for PEG/GOX. This means that inclusion of AuNPs improved conductivity of PEG hydrogels by a factor of 5. Overall, our results indicate that incorporating AuNPs enhances electron transfer and increases conductivity of the hydrogel. Importantly, as shown in Figure 3D, loading of AuNP into the gel affected conductivity of the gel. Higher loading of NPs resulted in lower impedance (better conductivity).

3.3 Detection of Glucose and Hydrogen Peroxide Using Nanocomposite Hydrogel Electrodes

After determining AuNP-carrying hydrogels to be more conductive, we characterized catalytic properties of enzyme molecules entrapped in the hydrogel alongside nanoparticles. Figure 4A shows the cyclic voltammograms from hydrogel-modified electrode containing PEG/AuNP/GOX as well as vinylferrocene (VF) – a redox mediator.

These electrodes exhibited anodic and cathodic peaks at 0.35 and 0.25 V (vs. Ag/AgCl) that were consistent with ferrocene redox peaks. Importantly, anodic peak has increased in response to addition of glucose aliquots – suggesting electrocatalytic oxidation of the substrate. Figure 4B shows the cyclic voltammograms obtained from AuNP/GOX-containing electrodes in the absence of VF. In this case electron transfer is likely mediated by AuNPs but may also be occurring by direct contact between the prosthetic group ($FAD/FADH_2$) of GOX and the electrode surface [32]. The anodic current once again increased as varying concentrations of glucose were introduced into the system. However, comparison of Figures 4A and B shows that VF-containing nanocomposite hydrogels had ca. 3 times higher current density than hydrogels without this redox mediator (see Figure 4C). This result suggests that inclusion of VF either increases conductivity of electrons through the gel or improves electron transfer from the enzyme molecules.

The oxidation of glucose at GOX/AuNP containing electrodes was studied by amperometry. Figure 5A shows typical amperometric responses of a sensing electrode poised at 0.35 V and challenged with successive additions of 0.1 mM glucose in 1xPBS. Immediately after adding glucose, the current increases and 90% of the signal is reached after ca. 5 s. This indicates an excellent response time for PEG/AuNP/GOX electrode. The calibration curve of the glucose vs. current reveals that glucose biosensor has sensitivity of $100\ \mu A\,M^{-1}\,cm^{-2}$. The detection limit – defined as the value of the signal three times above the noise – was estimated to be 3.7×10^{-7} M. As highlighted by Table 1, this limit of detection is comparable to some of the most sensitive glucose biosensors reported in the literature. Figure 5B describes responses of AuNP/GOX-containing hydrogel biosensors to higher glucose concentrations and demonstrates that the linear range of the biosensor extended to 10 mM glucose. While sensing experiments presented here were carried out in deoxygenated buffer, we have previously shown that electrochemical biosensor based on VF and GOX molecules encapsulated into hydrogels was insensitive to oxygen tension. Therefore, we envision being able to use this type of a biosensor in situations where oxygen tension may vary (e.g. cell culture experiments).

In addition, we characterized responses of AuNP/HRP containing hydrogel biosensors to hydrogen peroxide. As with glucose detection, electrodes were poised at 0.35 V – the anodic potential of redox molecules (VF) incorporated into the gel alongside AuNP/HRP. This allowed us to operate in the voltage regime where oxidation of interfering species was minimal. Figure 5C shows the current vs. time response of nanocomposite hydrogel-coated electrodes that were challenged with 0.5 μM H_2O_2 additions in 1xPBS. The linear range of H_2O_2 spans 0.5 to 5.0 μM with a correlation coefficient of 0.98. The sensitivity was evaluated as the slope of the linear range of the calibration curve in the insert of Figure 5C. This value was determined to be $1.4\ mA\,M^{-1}\,cm^{-2}$. Limit of detection (defined

Table 1. Comparison of analytical performance of some glucose biosensors.

Glucose biosensor	Detection limit (μM)	Reference
PEG/AuNP/Gox	0.3	This work
GOx-polyacrylonitrile	20.0	[32]
GOx-sol–gel-chitosan	10.0	[33]
GOx-sol–gel-CNTs	50.0	[34]
Nafion-GOx-SWCNH	6.0	[35]
GOx-TEOS-sol–gel	200.0	[36]

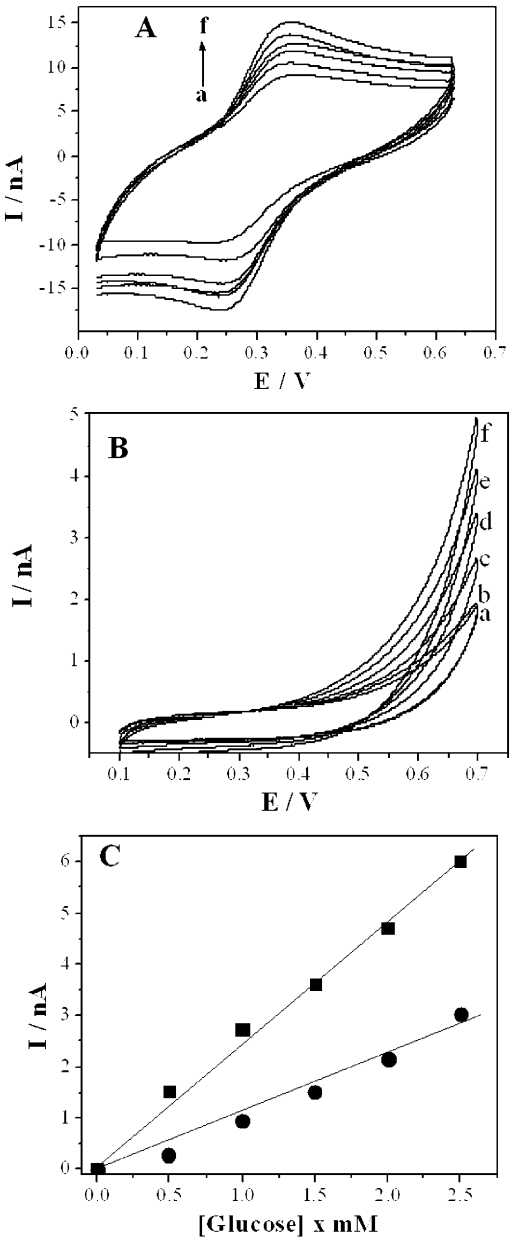

Fig. 4. A, B) Cyclic voltammetry analysis of sensing electrodes with (A) and without (B) vinylferrocene. Electrodes were challenged with following concentrations of glucose (a) 0 mM, (b) 0.5 mM, (c) 1.0 mM, (d) 1.5 mM, (e) 2.0 mM and (f) 2.5 mM. Experiments were carried out in 1x PBS at the scan rate of $30\ mV\,s^{-1}$. C) Calibration curves created by plotting anodic peak current vs. glucose concentration. Current values were chosen for $E = 0.35$ V (■) and 0.65 V (●).

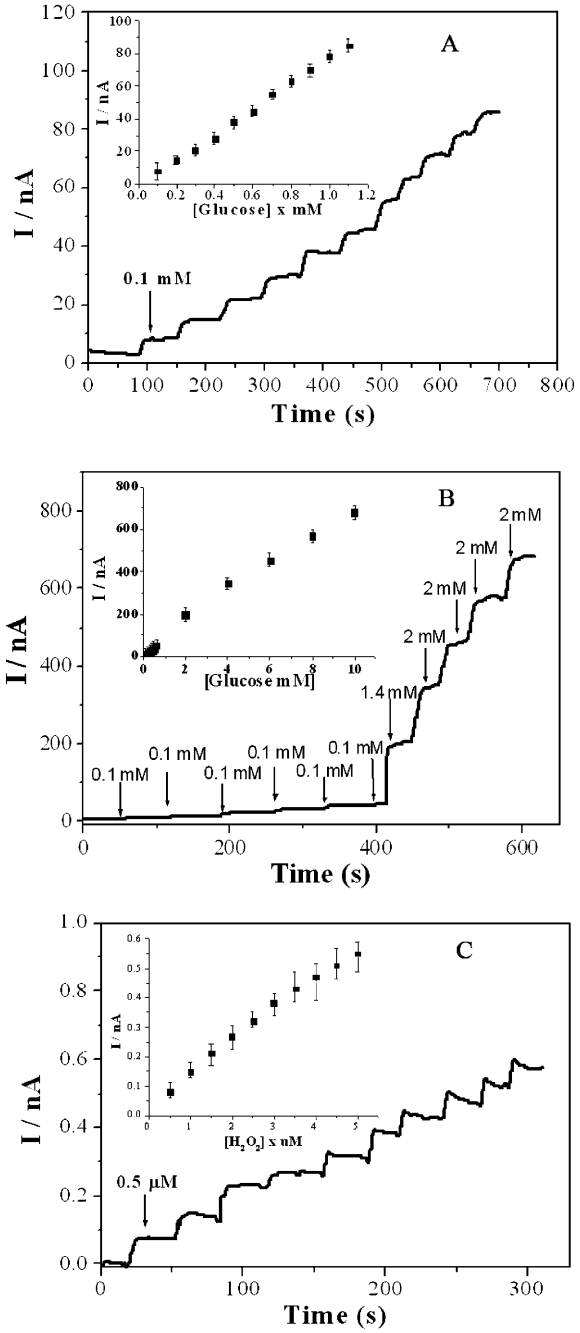

Fig. 5. A) Amperometric response of the PEG/AuNP/GOx biosensor to successive additions of 0.1 mM glucose in 1x PBS at an applied potential of +0.35 V vs. Ag/AgCl reference. Insert: calibration curve of amperometric responses vs. glucose concentration. This graph shows electrode responses to glucose in the concentration range from 0.1 to 1 mM. B) Amperometry experiments showing response to higher glucose concentration (up to 10 mM). Inset provides a calibration curve of current vs. analyte concentration. C) Response of AuNP/HRP/VF containing nanocomposite hydrogels to varying concentrations of H_2O_2. Sensing electrodes were challenged with 0.5 µM H_2O_2. Operating potential was 0.35 V. Inset: Calibration plots of current vs. analyte concentration.

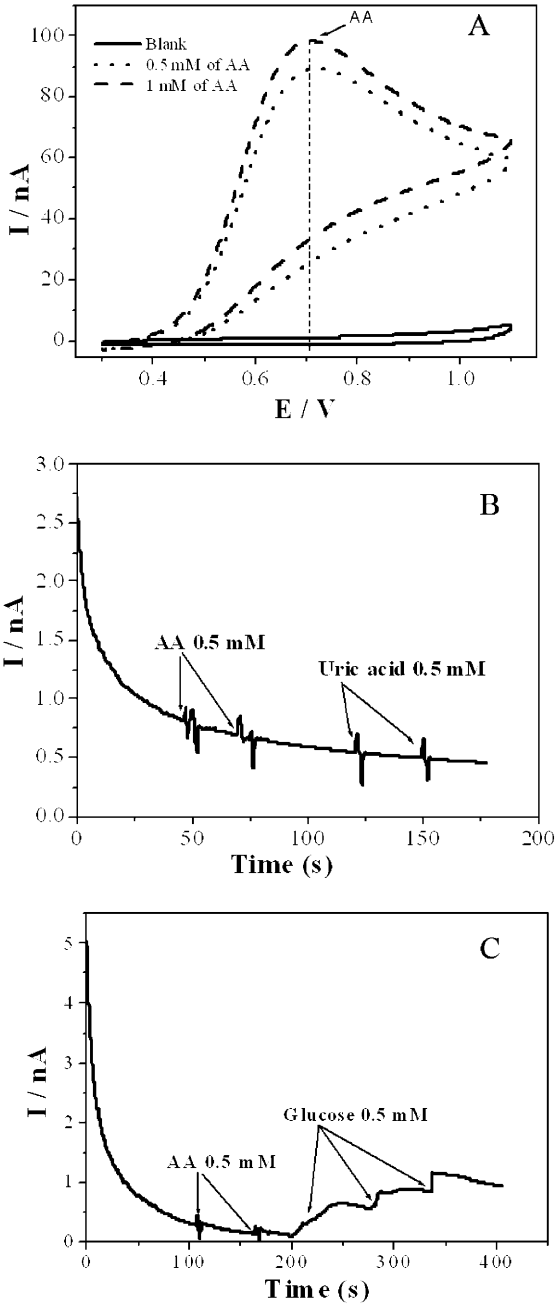

Fig. 6. A) Cyclic voltammetry in the presence of interfering compounds: uric acid (UA) and ascorbic acid (AA). Scan rate was 30 $mV s^{-1}$. This result shows significant oxidation at 0.7 V but minimal oxidation below 0.4 V vs. Ag/AgCl reference. B, C) Amperometry results where nanocomposite hydrogel/Au electrodes were poised at 0.35 V vs. Ag/AgCl references challenged with UA and AA. Sensing electrodes did not respond to these substances (B) but did respond to glucose (C), demonstrating specificity of the glucose biosensor.

as signal three times above noise) was calculated to be 51 nM.

3.4 Specificity to Glucose in the Presence of Interfering Substances

Small molecules such as ascorbic acid (AA) and uric acid (UA) are present in physiological fluids and can be oxidized at the electrode, thus masking sensor response to

glucose or hydrogen peroxide. We investigated the effects of 0.5 mM AA and UA on the glucose sensor response at anodic potentials. Figure 6A shows CV of AA oxidation at nanocomposite hydrogel/Au electrode. As seen from this experiment, oxidation was at its highest at 0.7 V and became negligible below 0.4 V. Poising the electrode at 0.35 V and introducing 0.5 mM AA and UA did no result in appreciable oxidation currents (see Figure 6B). In comparison, addition 0.5 mM glucose produced a strong jump in current pointing to breakdown of glucose by GOX (see Figure 6C). These results demonstrate that electrodes functionalized with nanocomposite hydrogels were selective to glucose in the presence of other interfering substances.

4 Conclusions

This paper describes the development of electrochemical biosensors using AuNP encapsulation into hydrogel microstructures. Photolithography-like process was used to functionalize Au electrode arrays with AuNP/enzyme-carrying hydrogel microstructures. Inclusion of AuNPs was found to enhance conductivity of PEG hydrogels by 5 fold. Conjugation of GOX molecules to AuNP and encapsulation of these conjugates in PEG hydrogel microstructures allowed to construct biosensors with glucose sensitivity of 100 $\mu A\,mM^{-1}\,cm^{-2}$ and lower detection limit of 0.3 μM. Inclusion of AuNPs made this nanocomposite hydrogel-based biosensor 100 times more sensitive than our previous hydrogel-based glucose sensor that did not contain AuNP.[23] Importantly, sensitivity and detection of limit of the glucose biosensor described here approaches some of the best glucose biosensors reported in the literature.

While AuNPs have seen extensive use in biosensor development, our paper is one of the first to describe encapsulation of enzyme-functionalized AuNPs inside nonfouling PEG hydrogels and micropatterning of these nanocomposite hydrogels on microelectrode arrays. In the future, we envision utilizing excellent nonfouling properties and sensitivity of these nanocomposite biosensors for monitoring analytes in cell cultures or complex biological fluids such as blood.

Acknowledgements

The financial support for this study was provided by grants (NIH CA126716) and NSF (EFRI #0937997) awarded to AR. Additionally, ALS acknowledges working at the *National Science Foundation* during the time this study was carried out. The views expressed in this article are those of the authors, and do not reflect the views of the *National Science Foundation*.

References

[1] M. Bui, S. Lee, K. Han, X. Pham, C. Li, J. Choo, G. Seong, *Chem. Commun.* **2009**, 5549.
[2] W. Cai, Q. Xu, X. Zhao, J. Zhu, H. Chen, *Chem. Mater.* **2006**, *18*, 279.
[3] A. Shipway, M. Lahav, I. Willner, *Adv. Mater.* **2000**, *12*, 993
[4] Y. Xiao, F. Patolsky, E. Katz, J. Hainfeld, I. Willner, *Science* **2003**, *299*, 1877.
[5] G. Mor-Piperberg, R. Tel-Vered, J. Elbaz, I. Willner, *J. Am. Chem. Soc.* **2010**, *132*, 6878.
[6] I. Willner, B. Basnar, B. Willner, *FEBS J.* **2007**, *274*, 302.
[7] O. Lioubashevski, V. Chegel, F. Patolsky, E. Katz, I. Willner, *J. Am. Chem. Soc.* **2004**, *126*, 7133.
[8] X. Luo, J. Xu, Q. Zhang, G. Yang, H. Chen, *Biosens. Bioelectron.* **2005**, *21*, 190.
[9] S. Phadtare, A. Kumar, V. Vinod, C. Dash, D. Palaskar, M. Rao, P. Shukla, S. Sivaram, M. Sastry, *Chem. Mater.* **2003**, *15*, 1944.
[10] M. Daniel, D. Astruc, *Chem. Rev.* **2004**, *104*, 293.
[11] J. Jagur-Grodzinski, *Pol. Adv. Tech.* **2010**, *21*, 27.
[12] P. Schexnailder, G. Schmidt, *Colloid. Pol. Sci.* **2009**, *287*, 1.
[13] I. Tokarev, I. Tokareva, S. Minko, *Adv. Mater.* **2008**, *20*, 2730.
[14] J. O. You, D. T. Auguste, *Langmuir* **2010**, *26*, 4607.
[15] W. Chen, C. Li, P. Chen, C. Sun, *Electrochim. Acta* **2007**, *52*, 2845.
[16] W. Lee, R. Scholz, K. Niesch, U. Gosele, *Angew. Chem.-Int. Ed.* **2005**, *44*, 6050.
[17] W. G. Koh, M. Pishko, *Sens. Actuators B* **2005**, *106*, 335.
[18] A. Revzin, R. J. Russell, V. K. Yadavalli, W. G. Koh, C. Deister, D. D. Hile, M. B. Mellott, M. V. Pishko, *Langmuir* **2001**, *17*, 5440.
[19] R. J. Russell, M. V. Pishko, C. G. Gefrides, M. J. Mcshane, G. L. Cote, *Anal. Chem.* **1999**, *71*, 3126.
[20] C. P. Quinn, C. P. Pathak, A. Heller, J. A. Hubbell, *Biomaterials* **1995**, *16*, 389.
[21] P. D. Drumheller, J. A. Hubbell, *J. Biomed. Mater. Res.* **1995**, *29*, 207.
[22] A. Revzin, R. G. Tompkins, M. Toner, *Langmuir* **2003**, *19*, 9855.
[23] J. Yan, V. A. Pedrosa, A. L. Simonian, A. Revzin, *Acs Appl. Mater. Int.* **2010**, *2*, 748.
[24] M. V. Pishko, A. C. Michael, A. Heller, *Anal. Chem.* **1991**, *63*, 2268.
[25] S. A. Merchant, T. O. Tran, M. T. Meredith, T. C. Cline, D. T. Glatzhofer, D. W. Schmidtke, *Langmuir* **2009**, *25*, 7736.
[26] X. Wang, L. Li, B. Van der Meer, J. Jin, D. Tang, Z. Hui, Y. Li, T. Li, *Biochem. Biophys. Acta* **2001**, *1544*, 333.
[27] D. Li, Q. He, Y. Cui, L. Duan, J. Li, *Biochem. Biophys. Res. Commun.* **2007**, *355*, 488.
[28] N. Nath, A. Chilkoti, *Anal. Chem.* **2002**, *74*, 504.
[29] D. Hobara, Y. Uno, T. Kakiuchi, *Phys. Chem. Chem. Phys.* **2001**, *3*, 3437.
[30] Y. Feng, T. Yang, W. Zhang, C. Jiang, K. Jiao, *Anal. Chim. Acta* **2008**, *616*, 144.
[31] V. Pardo-Yissar, R. Gabai, A. Shipway, T. Bourenko, I. Willner, *Adv. Mater.* **2001**, *13*, 1320.
[32] H. Zheng, H. Xue, Y. Zhang, Z. Shen, *Biosens. Bioelectron.* **2002**, *17*, 541.
[33] X. Chen, J. Jia, S. Dong, *Electroanalysis* **2003**, *15*, 608.
[34] A. Salimi, R. G. Compton, R. Hallaj, *Anal. Biochem.* **2004**, *333*, 49.
[35] X. Liu, L. Shi, W. Niu, H. Li, G. Xu, *Biosens. Bioelectron.* **2008**, *23*, 1887.
[36] E. Forzani, H. Zhang, L. Nagahara, I. Amlani, R. Tsui, N. Tao, *Nano Lett.* **2004**, *4*, 1785.

